Faraday-rotation spectra of semimagnetic semiconductors

S. Hugonnard-Bruyère, C. Buss, F. Vouilloz, R. Frey, and C. Flytzanis
Laboratoire d'Optique Quantique, Ecole Polytechnique, 91128 Palaiseau Cedex, France
(Received 23 February 1994; revised manuscript received 25 April 1994)

An analytical expression of the Verdet constant of semimagnetic semiconductors is derived from a microscopic analysis of the transverse susceptibility responsible for the Faraday effect. This expression is obtained by integrating, in k space, the wave-vector-dependent transverse polarizability. The latter is obtained within the density-matrix formalism using a Lorentzian shape for the wave-vector dependence of the exchange interaction. Using only two parameters, this model reproduces very well the experimental Faraday-rotation spectra available for both $Cd_{1-x}Mn_xTe$ and $Zn_{1-x}Mn_xTe$ for various manganese concentrations and sample temperatures. The normalization parameter is independent of the manganese concentration and sample temperature for a given type of semimagnetic semiconductor, and the same exchange parameter is used for all manganese concentrations at a given temperature. Using the experimental data obtained in $Cd_{1-x}Mn_xTe$ samples of precisely known manganese concentrations, we are able to extract the value $q=0.022$ at 77 K and $q=0.018$ at 290 K for the exchange interaction parameter with a relative precision of 5%, while for $Zn_{1-x}Mn_xTe$ a smaller value ($q=0.003$ at room temperature) is obtained from previous studies.

I. INTRODUCTION

Semimagnetic semiconductors (SMSC's) represent a class of materials that exhibit many striking and technologically useful properties, especially when placed inside a magnetic field.[1,2] Among these properties, the strong spin-spin–exchange interaction occurring between the d electrons of the Mn^{2+} ions and the s-like conduction-band and p-like valence-band electrons[3] profoundly affects all physical phenomena that depend on the Zeeman splitting of the band sublevels. For instance, this spin-spin–exchange interaction leads to the well-known giant Faraday rotation observed at photon energies E near the band-gap resonance.[4,5] The effect has been subsequently studied in various SMSC's, in particular, in the optically isotropic $Cd_{1-x}Mn_xTe$ and $Zn_{1-x}Mn_xTe$.[6–10]

Following Bartholomew, Furdyna, and Ramdas,[7] several authors have analyzed the Faraday-rotation spectra in terms of a single-oscillator model for the refractive index that involves the interband excitonic transition at the fundamental gap E_g. This model reproduces very well the dependence in $(1-E/E_g)^{-3/2}$ of the Faraday-rotation spectrum near the band-gap resonance, but as pointed out by Jiménez-González, Aggarwal, and Becla,[10] it is based on an inappropriate assumption, namely, that the value of the refractive index is dominated by the excitonic transition at the fundamental gap. A two-oscillator model introduced to explain the Faraday-rotation spectra especially in the infrared region of the spectrum[10] also provides satisfactory fits for the Faraday-rotation spectra but requires two independent parameters for each spectrum measured at a given Mn^{2+} concentration and sample temperature.

The effective oscillator models, however, fail to establish a direct connection with the microscopic origin of the Zeeman effect responsible for the Faraday rotation. On the other hand, in nonmagnetic II-VI semiconductors, such a microscopic approach explicitly taking into account the k-wave-vector dependence of the valence and conduction bands was used[11,12] and this approach predicted a resonance behavior for the Faraday-rotation angle θ_L proportional to $(1-E/E_g)^{-1/2}$. This model was successfully applied to several large band-gap II-VI semiconductors such as ZnS, ZnSe, CdS, and ZnTe.[13]

In the following, we extend this model to the case of SMSC's by adding the spin-spin–exchange interaction to the pure Zeeman effect in the magnetic-field-dependent splitting of the spin sublevels of each $|\mathbf{k}\rangle$ state in the Brillouin zone. Moreover, following Bhattacharjee,[14] we use an explicit wave-vector dependence for the spin-spin–exchange interaction in semimagnetic semiconductors. This model, where the k dependence of the exchange interaction plays a crucial role, explains very well experimental results obtained in SMSC's for various Mn^{2+} concentrations by using only two parameters for a given type of SMSC's.

II. THEORETICAL BACKGROUND

In order to discuss Faraday rotation, let us consider a monochromatic light beam of frequency $\omega[\mathcal{E}(z,t)=\mathbf{E}(\omega)\exp i(kz-\omega t)+\text{c.c.}]$ traveling through an optically isotropic crystal along an external magnetic field $\mathbf{H}$ parallel to $\hat{\mathbf{z}}$ where $\hat{\mathbf{x}}$, $\hat{\mathbf{y}}$, and $\hat{\mathbf{z}}$ define a right-handed coordinate system. Faraday-rotation results from the difference in phase velocity of right $[\hat{\sigma}_-=1/\sqrt{2}(\hat{\mathbf{x}}-i\hat{\mathbf{y}})]$ and left $[\hat{\sigma}_+=1/\sqrt{2}(\hat{\mathbf{x}}+i\hat{\mathbf{y}})]$ circularly polarized light waves propagating through the medium along $\mathbf{H}$. The Faraday-rotation angle θ_F is then given by

$$\theta_F=\frac{EL}{2\hbar c}(n_- - n_+)\ , \tag{1}$$

where $E=\hbar\omega$ is the photon energy, L is the crystal

length, c is the light velocity in vacuum, and n_- and n_+ are the refractive indices for $\hat{\sigma}_-$ and $\hat{\sigma}_+$ polarizations, respectively. For an optically isotropic magnetic crystal, the permittivity tensor $\underline{\varepsilon}$ is given by[15]

$$\underline{\varepsilon}=\begin{bmatrix}\varepsilon_0 & \varepsilon_{xy} & 0\\ -\varepsilon_{xy} & \varepsilon_0 & 0\\ 0 & 0 & \varepsilon_0\end{bmatrix}, \tag{2}$$

where $\varepsilon_0=n_0^2$ and n_0 is the refractive index without magnetic field. In Eq. (2), ε_{xy} is the magnetic-field-dependent transverse permittivity responsible for the Faraday-rotation effect. Taking into account the relation $\underline{\varepsilon}=\underline{1}+4\pi\underline{\chi}$ existing between $\underline{\varepsilon}$ and the susceptibility tensor $\underline{\chi}$, the Faraday-rotation angle may be written as

$$\theta_F=-i\frac{2\pi EL}{\hbar c n_0}\chi_{xy}(E)\ , \tag{3}$$

where $\chi_{xy}(E)$ is the transverse part of $\underline{\chi}$, which naturally depends on the light photon energy E. Note that Eq. (3) is obtained under the valid approximation $|\varepsilon_{xy}|\ll\varepsilon_0$, which is the opposite of that taken in Ref. 7. $\chi_{xy}(E)$ is calculated using the microscopic theory of susceptibilities[16] and is obtained through the summation of the polarizability over all the possible quantum states. At very high magnetic fields H and low temperatures T, the cyclotron-resonance frequency ω_c is large ($\hbar\omega_c\gg k_BT$), and the Landau quantization must be taken into account in order to describe the quantum states of electrons.[17] On the contrary, at the moderate magnetic fields ($H<10$ T) and temperatures ($T>3$ K), which correspond to most experimental situations, the Landau levels are removed by collisions and $\chi_{xy}(E)$ is simply given by

$$\chi_{xy}(E)=\frac{1}{2\pi^2}\int_0^\infty k^2\alpha_{xy}(k,E)dk\ , \tag{4}$$

where $\alpha_{xy}(k,E)$ is the polarizability at the photon energy E for electrons of wave vector $\mathbf{k}$.

Using the microscopic theory of polarizabilities,[16] $\alpha_{xy}(k,E)$ is given by

$$\alpha_{xy}(k,E)=\sum_{n,n'}(\rho^{(0)}_{nn}-\rho^{(0)}_{n'n'})\frac{\langle n'|P_x|n\rangle\langle n|P_y|n'\rangle}{E-(E_n-E_{n'})}\ , \tag{5}$$

where the summation (n,n') is performed over all the spin sublevels for a given k state in the valence and conduction bands. In Eq. (5), which is valid only out of resonance, $\rho^{(0)}_{mm}$ and $E_m(m=n,n')$ are the occupancy probability and energy of the level considered, and $P_x(P_y)$ is the projection of the dipolar electric operator on the $\hat{x}$ ($\hat{y}$) axis. Introducing the projection $P_\pm=1/\sqrt{2}(P_x\pm iP_y)$ of the dipolar electric operator on the $\hat{\sigma}_\pm$ polarizations, $\alpha_{xy}(k,E)$ is given by

$$\alpha_{xy}(k,E)=i\frac{\hbar^2e^2E}{2m}\sum_{n,n'}\frac{\rho^{(0)}_{nn}}{E_{n'n}(E^2_{n'n}-E^2)}[f^{(+)}_{n'n}-f^{(-)}_{n'n}] \tag{6}$$

with

$$f^{(\pm)}_{n'n}=\frac{2m}{\hbar^2e^2}E_{n'n}|\langle n|P_\pm|n'\rangle|^2\ ,$$

where $E_{n'n}=E_{n'}-E_n$ and e and m are charge and mass of electrons, respectively. For a zinc-blend-type crystal, the states involved in Eq. (6) are $|m\rangle=|v,\mathbf{k},\pm s/2\rangle$ ($m=n',n$ and $s=1,3$) in the valence band and $|m\rangle=|c,\mathbf{k},\pm\frac{1}{2}\rangle$ ($m=n',n$) in the conduction band (see Fig. 1, where the transitions allowed in the Faraday configuration are also shown). Assuming that the oscillator strengths $f^{(\pm)}_{n'n}$ are independent on k and H,[18] and noting that

$$|\langle\pm\tfrac{3}{2}|P_\mp|\pm\tfrac{1}{2}\rangle|^2=3|\langle\pm1/2|P_\mp|\mp|\tfrac{1}{2}\rangle|^2$$

(Ref. 3), $\alpha_{xy}(k,E)$ is given by

$$\alpha_{xy}(k,E)=\frac{i}{3}EE_gd^2\sum_{s=1,3}[J(s)-J(-s)]\ , \tag{7}$$

where E_g and d are the gap energy and transition dipole moment at $k=0$, respectively, and $J(s)$ is given by

$$J(s)=|s|\frac{\tilde{\rho}_v\left[k,\frac{s}{2}\right]-\tilde{\rho}_c\left[k,\frac{\varepsilon}{2}\right]}{\Delta E(k,s)[\Delta E^2(k,s)-E^2]} \tag{8}$$

with $\Delta E(k,s)=E_c(k,\varepsilon/2)-E_v(k,s/2)$; $\tilde{\rho}_v(k,s/2)$ and $\tilde{\rho}_c(k,\varepsilon/2)$ are the occupancy probabilities of the $|v,\mathbf{k},s/2\rangle$ and $|c,\mathbf{k},\varepsilon/2\rangle$ spin sublevels in the valence and conduction bands, respectively, and we have $\varepsilon=\pm1$

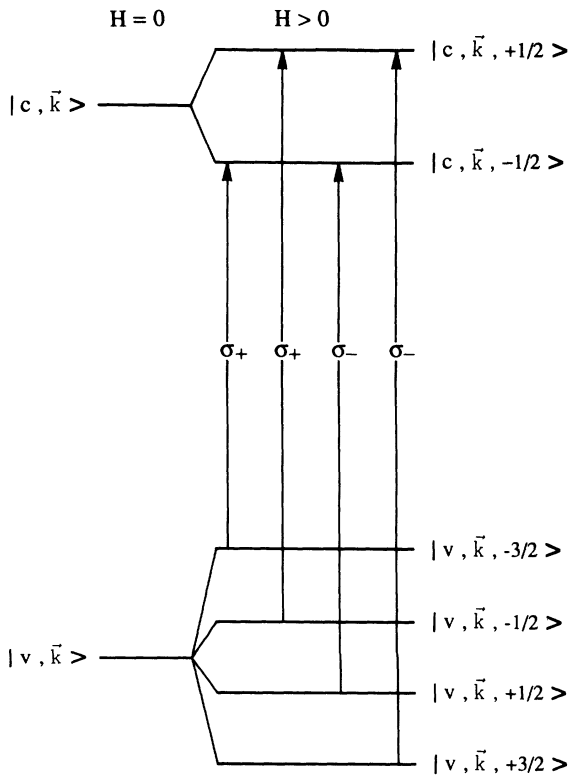

FIG. 1. Schematic illustration of the transitions between the spin-split valence- and conduction-band sublevels $|\mathbf{k}\rangle$ in the Faraday configuration.

(∓ 1) for $s=\pm 3$ (± 1), respectively. The energies of the spin sublevels in the conduction and valence bands are given by

$$E_c\left[k,\frac{\varepsilon}{2}\right]=E_g+\frac{\hbar^2k^2}{2m_c}+\frac{\varepsilon}{2}[-g_c\mu_B H+AM]\ , \tag{9a}$$

and

$$E_v\left[k,\frac{s}{2}\right]=-\frac{\hbar^2k^2}{2m_{v_s}}-\frac{s}{2}[g_{v_s}\mu_B H+\tfrac{1}{3}BM]\ , \tag{9b}$$

where m_c and m_{v_x} are the effective masses of electrons and holes in the conduction and valence bands [light $(s=1)$ and heavy $(s=3)$ electrons], respectively, g_c and g_{v_s} are the Landé factors of electrons in the conduction and light $(s=1)$ and heavy $(s=3)$ valence bands, respectively, $\mu_B=0.927\times 10^{-20}$ erg/G being the Bohr magneton. In Eqs. (9a) and (9b) the terms AM and $BM/3$ are introduced to take the exchange interaction into account, M being the magnetization of Mn^{2+} ions, and A and B being given by

$$A=\frac{\alpha}{g_{\mathrm{Mn}}\mu_B}\frac{k_0^2}{k^2+k_0^2}\ , \tag{10a}$$

and

$$B=\frac{-\beta}{g_{\mathrm{Mn}}\mu_B}\frac{k_0^2}{k^2+k_0^2}\ , \tag{10b}$$

where g_{Mn} is the Landé factor of Mn^{2+} ions and α and $-\beta$ are the values per atom of the exchange integrals in the conduction and valence bands, respectively.[19] For the sake of simplicity, the wave-vector dependence of the exchange interaction[14] is taken into account in Eqs. (10) by the Lorentzian factor $k_0^2/(k_0^2+k^2)$, where k_0 is a fitting parameter.

Note that such a wave-vector dependence of the exchange interaction was already observed, for instance, in $Cd_{1-x}Mn_xTe$, the pseudo-Zeeman splitting being 16 times smaller at the L point in the Λ direction than at the Γ point near the band-gap resonance of the semiconductor.[20] It is also important to anticipate here that this k dependence of the exchange interaction is essential in obtaining a good agreement with experimental results. Indeed, when this k dependence is not taken into account, the analytical solution exhibits a resonance in $(1-E/E_g)^{-1/2}$ near the band-gap resonance[21] instead of the $(1-E/E_g)^{-3/2}$ behavior experimentally observed.[7]

At high temperatures (typically $T>60$ K) the magnetization can be linearized in[22]

$$M=\frac{xN_0(g_{\mathrm{Mn}}\mu_B)^2S(S+1)}{3k_B[T-\theta(x)]}H\ , \tag{11}$$

where N_0 is the total density of cation sites, $S=\frac{5}{2}$ is the spin of the Mn^{2+} ions, and $\theta(x)=\theta_0 x$ with x the Mn^{2+} concentration. The constant θ_0 has the values -470 and -831 K for $Cd_{1-x}Mn_xTe$ and $Zn_{1-x}Mn_xTe$, respectively.[22]

The Faraday-rotation angle θ_F is then calculated for large gap semiconductors $[\tilde{\rho}_v(k,s/2)=1$ and $\tilde{\rho}_c(k,\varepsilon/2)=0]$ by analytically performing the integration in Eq. (4). Since in the temperature and magnetic field ranges considered θ_L is proportional to H, we use the Verdet constant $V(E)=\theta_L/(LH)$ whose expression is obtained as

$$V(E)=Zf(X)+CYg(X) \tag{12}$$

with $X=E/E_g$ and

$$Z=\frac{d^2E_g^{1/2}}{4\hbar cn_0}\left[\frac{2m_3}{\hbar^2}\right]^{3/2}\times\mu_B\left[(3g_3-g_c)+\frac{1}{3}(g_1+g_c)\left[\frac{m_1}{m_3}\right]^{3/2}\right]\ , \tag{13}$$

$$C=\frac{d^2E_g}{24\hbar cn_0}\left[\frac{2m_3}{\hbar^2}\right]^{3/2}(N_0\alpha-N_0\beta)\frac{g_{\mathrm{Mn}}\mu_B S(S+1)}{k_B}\ , \tag{14}$$

and

$$Y=\frac{Q}{E_g^{1/2}}\frac{x}{T-\theta_0 x}\ , \tag{15}$$

where $m_j^{-1}=m_c^{-1}+m_{v_j}^{-1}$ $(j=1,3)$ and $Q=qE_{g_0}/E_g$ with $q=\hbar^2k_0^2/(2m_3E_{g_0})$, E_{g_0} being the gap energy of CdTe at 77 K used as an energy reference.

The photon energy dependence of the Verdet constant is given by $f(X)$ and $g(X)$ for the pure Zeeman and exchange contributions, respectively, with

$$f(X)=\frac{1}{(1+X)^{1/2}}+\frac{1}{(1-X)^{1/2}}-2\ , \tag{16}$$

$$g(X)=-\left[\frac{1}{(1+X)^{1/2}[(1+X)^{1/2}+Q^{1/2}]^2}+\frac{1}{(1-X)^{1/2}[(1-X)^{1/2}+Q^{1/2}]^2}-\frac{2}{[1+Q^{1/2}]^2}\right]\ . \tag{17}$$

As shown hereafter, when $V(E)$ is given by Eq. (12), the constant C which contains the oscillator strength (d^2E_g) and exchange integrals $(N_0\alpha-N_0\beta)$ depends neither on the Mn^{2+} concentration nor on the sample temperature.

In Eqs. (12)–(17) we have neglected the small light-hole contribution which is proportional to $\frac{1}{3}(N_0\alpha+N_0\beta/3)(m_1/m_3)^{3/2}$ and is, therefore, less than 1% of the heavy-hole contribution $(N_0\alpha-N_0\beta)$. It is also important to note that the results given by Eqs. (12)–(17) are valid only if the light frequency is not too close to the band-gap resonance, or equivalently for

$$1-X\gg\left[2Q\frac{(A+B)M}{E_g}\right]^{-1/2}\ , \tag{18}$$

where $(A+B)M$ represents the maximum spin-exchange interaction-induced Zeeman splitting for a SMSC placed

in the magnetic field H at the temperature T.

For small values of Q ($Q \ll 1-X$), $g(X)$ reduces to

$$g'(X)=-\left[\frac{1}{(1+X)^{3/2}}+\frac{1}{(1-X)^{3/2}}-2\right] \tag{19}$$

which leads to the same resonance form in $(1-X)^{-3/2}$ as the experimental results and has, as expected, a sign which is opposite to that of the pure Zeeman contribution $f(X)$. Let us also remark that at very low frequencies ($X \ll 1$), $f(X)$ and $g'(X)$ reduce to $3X^2/4$ and $-15X^2/4$, respectively. The X^2 dependence of these functions is a supplementary indication of the validity of our analysis in this frequency range.[11,12]

III. EXPERIMENTAL RESULTS AND DISCUSSION

Experiments were performed in single crystals of $Cd_{1-x}Mn_xTe$ grown using either the Bridgeman ($x \sim 0$ and 0.03) or the traveling heater ($x \sim 0.10$ and 0.25) method.[23] The Mn^{2+} concentration of the three samples used was determined from electron beam-induced atomic emission in the x-ray range by the Laboratoire de Physique du Solide de Bellevue du CNRS in Meudon (France) at (3.3±0.3 %), (9.7±0.3 %), and (24.8±0.3 %). The samples were placed inside a magnetic cryostat providing temperatures between 3 and 300 K and magnetic fields up to 5 T. Faraday-rotation measurements were performed by using glan-prism polarizers. The light source was a cw Ar-laser-pumped Ti-sapphire laser in the range 1.18–1.82 eV and a BBO optical parametric generator amplifier pumped by the third harmonic of a single pulse (30 ps duration) delivered by a mode-locked Nd-YAG laser, where YAG denotes yttrium aluminum garnet, in the range 0.50–1.20 eV.[24] All the Faraday-rotation angles measured in these experiments were corrected from the small Faraday rotation of the windows of the cryostat.

Experiments were performed in pure CdTe samples in order to determine the constants entering in the pure Zeeman contribution to $V(E)$, since the spin-exchange interaction is absent in this case. Figure 2 shows the Verdet constant as a function of photon energy for two CdTe samples of different origins at 77 K (open squares and circles, for samples 1 and 2 respectively, in Fig. 2) and for the sample 1 at room temperature (open diamonds in Fig. 2). The data cannot be fitted satisfactorily by Eq. (12) with $x=0$ when using the values $E_{g_{CdTe}}=1.528$ and 1.596 eV at room and nitrogen temperature, respectively.[25] This discrepancy, already noticed by Atsuko Ebina, Takao Ko, and Shigeo Shionoya,[26] could be due to a negative contribution to $V(E)$ which would be more resonant than that of the band electrons. Note that this hypothesis is coherent with the sharp decrease of $V(E)$ observed near the band-gap resonance (see Fig. 2). However, good fits to experimental results were obtained by using Eq. (12) with $x=0$ when an effective value ($E'_{g_{CdTe}}$) was taken for the band-gap energy of CdTe. Indeed, in Fig. 2, the continuous lines represent the fits to experimental results obtained with the same $E'_{g_{CdTe}}=1.85$ eV for both temperatures. In order to obtain these fits we took $Z=10.7$ and 9.8 deg/kG/cm for $T=290$ and 77 K, respectively. As we are mostly interested in describing the exchange-interaction part of the Faraday-rotation effect, in the following X is replaced by $X'=XE_{g_{CdTe}}/E'_{g_{CdTe}}$ in $f(X)$ for describing the pure Zeeman contribution to $V(E)$ in cadmium manganese telluride. Note, however, that the fit is not valid for X greater than 0.94.

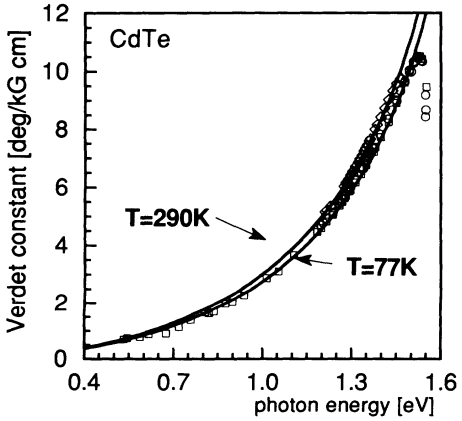

FIG. 2. Verdet dispersion for pure CdTe at 290 K (open diamonds) and 77 K (open squares and circles for two different samples).

Figures 3(a)–3(c) show the Verdet constant measured in $Cd_{1-x}Mn_xTe$ at 77 and 290 K for $x=0.033$, 0.097, and 0.248, respectively, as a function of the photon energy in the 1.20–1.90 eV range. In this figure, open circles and triangles correspond to measurements performed at 77 and 290 K, respectively. The continuous lines in Figs. 3(a)–3(c) are the fits obtained at the corresponding temperatures by using Eqs. (12)–(17). The gap energy appearing in these equations was calculated from the Mn^{2+} concentration by using the equation

$$E_g=(1-x)E_{g_{CdTe}}+xE_{g_{MnTe}} \tag{20}$$

with $E_{g_{CdTe}}=1.528$ and 1.596 eV ($E_{g_{MnTe}}=2.90$ and 3.05 eV) for CdTe (MnTe) at room and liquid-nitrogen temperature, respectively.[1] In these fits, the same value of $C=8.74\times10^5$ deg $eV^{1/2}$ K/(kG cm) was used for all experiments, thus confirming that this quantity depends neither on x nor on T. Moreover, the same value of q was taken at a given temperature whatever the Mn^{2+} concentration was ($q=0.022$ and 0.018 at 77 and 290 K, respectively). This indicates that the wave-vector dependence of the exchange interaction does not depend on the Mn^{2+} concentration as observed experimentally for the Zeeman splittings measured at the Γ and L points of the Brillouin zone.[20] On the contrary, as the value of q varies with the temperature, this k dependence of the exchange interaction slightly depends on T at least in the high-temperature regime of our experiments. In Figs. 3(b) and 3(c) the fits were stopped at $X=0.975$ in order to satisfy condition (18), while in Fig. 3(a) it was restricted to $X=0.94$ since the pure Zeeman contribution, which is relatively large in this low concentration case, is not fitted

correctly by our model for X larger than 0.94 (see Fig. 2). Note that, in our analysis, only three independent parameters are needed to fit the experimental results of six spectra of the Verdet constant and these, as seen in Fig. 3, are very good over a large frequency range.

Figure 4 shows the Verdet constant of $Cd_{1-x}Mn_xTe$ ($x=0.097$) at 77 K plotted as a function of the photon energy in the infrared region of the spectrum (0.6–1.2 eV). The experimental results (open circles in Fig. 4) are very well fitted by using exactly the same values $q=0.022$ and $C=8.74\times10^5$ for the free parameters as in Fig. 3. The very good quality of the fit demonstrates that our theory is also valid in the infrared region of the spectrum far from the band-gap resonance.

Figure 5 shows the Verdet constant in $Cd_{1-x}Mn_xTe$ ($x=0.097$) at 77 K plotted as a function of the photon energy in the resonant part of the spectrum with an expanded scale (1.5–1.7 eV). The open circles represent the experimental results and the three dotted, continuous, and broken lines are the fits obtained by using $q=0.012$, 0.022, and 0.032, respectively. These fits were obtained by adjusting the value of C in the infrared region of the spectrum in order to get a good fit in this spectral region. As the influence of q is significant only near the band-gap resonance [see Eqs. (12)–(17)], the fits provided exactly the same curve as the continuous line in Fig. 4 whatever the value of q was. As shown in Fig. 5, this is not the case near resonance, so that it was possible to determine q with a 5% relative precision ($q=0.022\pm0.001$). This indicates that the slight temperature dependence of the k dependence of the exchange interaction is real.

The resonance in $(1-X)^{-3/2}$ of the Verdet constant already observed experimentally when the spin-exchange interaction was preponderant[7] was also verified by plotting $[V(E)]^{-2/3}$ as a function of X for measurements per-

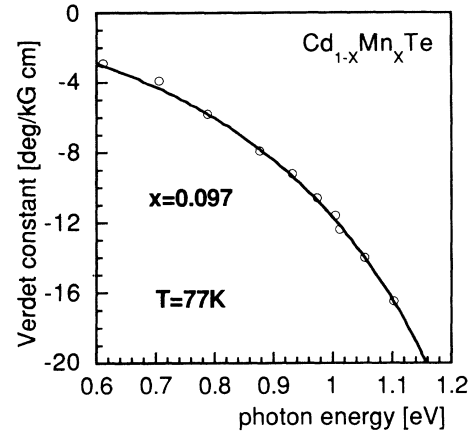

FIG. 4. Verdet dispersion for $Cd_{1-x}Mn_xTe$ ($x=0.097$) at 77 K in the infrared region of the spectrum. Solid line is the fit by our model.

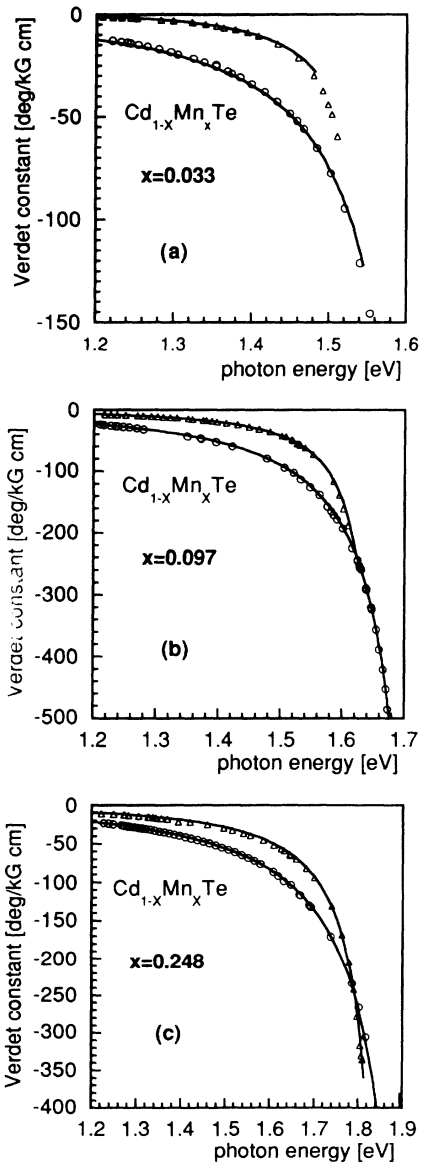

FIG. 3. Verdet dispersion for $Cd_{1-x}Mn_xTe$ at 290 K (open triangles) and 77 K (open circles) for three different Mn^{2+} concentrations: $x=0.033$, 0.097, and 0.248 in (a)–(c), respectively. Solid lines are the fits by our model.

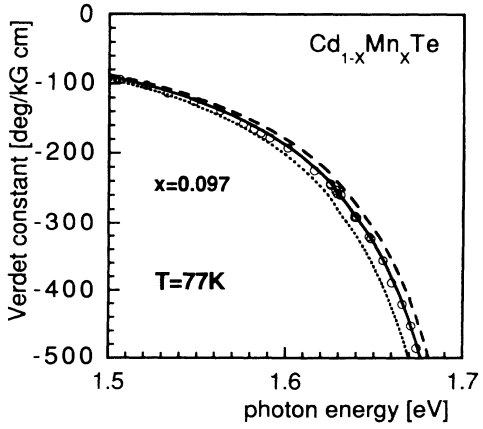

FIG. 5. Verdet dispersion for $Cd_{1-x}Mn_xTe$ ($x=0.097$) at 77 K near the band-gap resonance. Dotted, solid, and broken lines are the fits by our model with $q=0.012$, 0.022, and 0.032, respectively.

formed in $Cd_{1-x}Mn_xTe$ ($x=0.033$, 0.097, and 0.249) at liquid-nitrogen temperature. Results were similar for the different Mn^{2+} concentrations so that only those obtained for $x=0.097$ are plotted in Fig. 6. The experimental results (open circles in Fig. 6) which, naturally, are very well fitted through the use of Eq. (12) in the whole spectral range (continuous line in Fig. 6) can also be adequately described by a straight line (broken line in Fig. 6). Note, however, that this simplification is valid only in the limited range $X=0.85$ to 0.97, and that the intercept on the X axis is not obtained for $X=1$ but rather for $X=1.013$, this small difference being evidently related to the value of q.

Our model was also used to fit the experimental results obtained by other groups in $Cd_{1-x}Mn_xTe$, in particular, at room temperature.[7,9,10] The fits obtained with the same value $q=0.018$ (at 300 K) for the exchange parameter were all excellent, even at very low Mn^{2+} concentrations ($x=0.01$, for instance,[7]), provided that the values of C and x were sometimes slightly adjusted by less than 10%. These small discrepancies were probably due to small imprecisions, in particular, in the knowledge of x. Indeed, as shown in Fig. 7, good fits were obtained in the case of Ref. 10 with no adjustment of x which was precisely known. For $x=0.179$ and 0.268 the same value of C as in our experiments was used and a slightly different value [$C=7.50\times10^5$ deg $eV^{1/2}$ K/(kG cm)] was utilized for $x=0.076$, this small difference being possibly due to some imprecision in the sample thickness.

Our theoretical analysis was also applied to the case of $Zn_{1-x}Mn_xTe$. Figure 8 shows the experimental results obtained at room temperature by Bartholomew, Furdyna, and Ramdas,[7] together with the fits provided by our model (continuous lines). The curve for pure ZnTe ($x=0$) was obtained for $Z=10.7$ deg/kG/cm and $E_g=2.226$ eV which is only 2% smaller than the value $E_{g_{ZnTe}}=2.271$ eV measured by the exciton position.[27] This small difference proves that, contrary to the case of CdTe, the pure Zeeman effect is well accounted for by the model.[13,26] All the fits concerning $Zn_{1-x}Mn_xTe$ were obtained with the values of the constants ($C=4.35\times10^6$ deg $eV^{1/2}$ K/(kG cm) and $q=0.003$) by adjusting the Mn^{2+} concentration at the values 0.014, 0.039, 0.049, and 0.11 (see Fig. 8 for the corresponding curves). This represents relatively large changes when compared to the values assumed by the authors of Ref. 7 (0.02, 0.05, 0.05, and 0.10), but it is well known that in $Zn_{1-x}Mn_xTe$, due to the decrease of the liquidus temperature with increasing MnTe content in ZnTe, the Mn^{2+} concentration significantly increases from the lower tip of the ingot (first part to crystallize) to the higher one with a gradient concentration of about 3–5 %/cm.[28] This is, besides, confirmed by the very different results obtained by Bartholomew, Furdyna, and Ramdas for the Verdet constant of two samples of $Zn_{1-x}Mn_xTe$ having identical 0.05 nominal compositions (see the curves labeled $x=0.039$ and 0.049 in Fig. 8).

Note that our model can also describe very well results

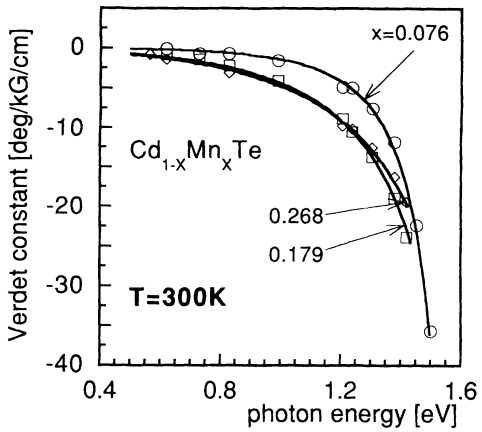

FIG. 7. Verdet dispersion for $Cd_{1-x}Mn_xTe$ at 300 K for various Mn concentrations, measured by Jimenez-Gonzalez, Aggarwal, and Becla (Ref. 10). Solid lines indicate the best fit by our model.

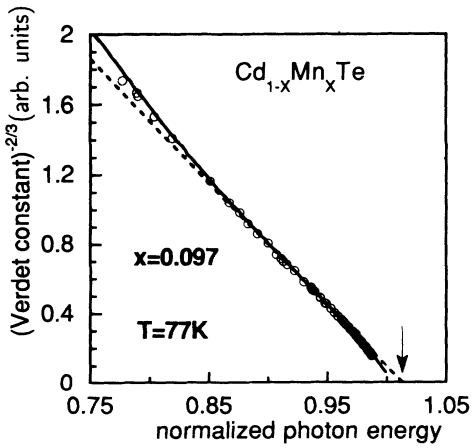

FIG. 6. Normalized Verdet dispersion for $Cd_{1-x}Mn_xTe$ ($x=0.097$) at 77 K illustrating the $(1-X)^{-3/2}$ dependence of $V(E)$. Solid line is the fit by our model. The broken straight line also fits the experimental results for $0.85<X<0.98$. The arrow shows the intercept of the straight line at $X=1.013$.

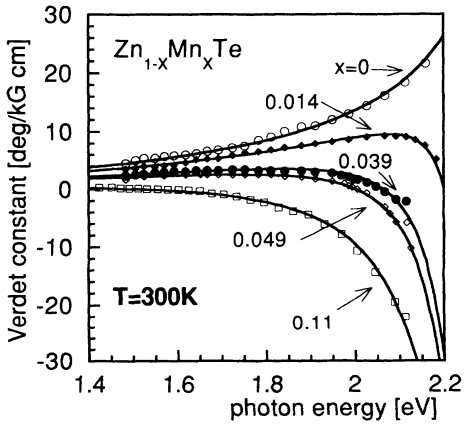

FIG. 8. Verdet dispersion for $Zn_{1-x}Mn_xTe$ at room temperature for several low values of x. Measurements by Bartholomew, Furdyna, and Ramdas are well fitted by our model (solid lines).

obtained at small values of the Mn^{2+} concentration. In particular, in the curve labeled $x=0.014$ in Fig. 8, the Verdet constant first increases with increasing frequencies far from the band-gap resonance where the pure Zeeman effect dominates before it decreases at higher frequencies when the most resonant exchange interaction overcomes the pure Zeeman effect.

Note also that, although the precision is worse for $Zn_{1-x}Mn_xTe$ ($q=0.003\pm0.002$ at room temperature for all values of x) than for $Cd_{1-x}Mn_xTe$ ($q=0.018\pm0.001$ at room temperature for all values of x), the role played by the exchange interaction in the splitting of the spin sublevels responsible for the Faraday effect decreases with increasing k faster in $Zn_{1-x}Mn_xTe$ than in $Cd_{1-x}Mn_xTe$. The same tendency was observed concerning the ratio of the Zeeman splitting at the Γ and L points which is $\frac{1}{16}$ for $Cd_{1-x}Mn_xTe$ (Ref. 20) and $\frac{1}{20}$ for $Zn_{1-x}Mn_xTe$.[29] However, it should be noted that the difference is less important in this case than in our measurements. This evidently suggests that the description of the wave-vector dependence of the exchange interaction by a simple Lorentzian, which seems convenient to fit the results of Faraday-rotation spectra, is probably not adequate in the whole Brillouin zone.

IV. CONCLUSION

In this work, an analytical formula has been obtained for the expression of the Verdet constant of semimagnetic semiconductors as a function of the Mn^{2+} concentration, sample temperature, and light frequency. This value was derived from the microscopic analysis of the transverse susceptibility responsible for the Faraday-rotation effect. In this analysis, the transverse susceptibility was obtained through the summation over the k wave vectors of the k-dependent transverse polarizability. The crucial point consisted in taking explicitly into account the k dependence of the spin–spin–exchange interaction, which was done by using a Lorentzian shape for the k-dependent exchange integrals. The model very well explains all experimental results available concerning Faraday-rotation spectra both in $Cd_{1-x}Mn_xTe$ and $Zn_{1-x}Mn_xTe$ for various Mn^{2+} concentrations and sample temperatures in large frequency ranges by using only normalization and exchange-interaction parameters provided the Mn^{2+} concentration is precisely known. The normalization parameter has been found to be independent of both the manganese concentration and sample temperature for a given type of semimagnetic semiconductor, and the same exchange parameter has been used for all x at a given temperature. Due to the effectiveness of our model the exchange-interaction parameter has been determined with a great precision in $Cd_{1-x}Mn_xTe$ ($q=0.022\pm0.001$ and $q=0.018\pm0.001$ at liquid nitrogen and room temperatures, respectively) by using our experimental results performed in samples of precisely known concentrations, and a reasonable value has been given in the case of $Zn_{1-x}Mn_xTe$ ($q=0.003\pm0.002$ at room temperature) where the manganese concentrations were not precisely known.

ACKNOWLEDGMENTS

The authors thank Dr. R. Triboulet from the Laboratoire de Physique du Solide de Bellevue du CNRS for valuable discussions and for providing them the high-quality $Cd_{1-x}Mn_xTe$ samples used in this experiment, as well as M. Rommeluere from the same Laboratory for the precise Mn^{2+} concentration measurements of the samples. This research was partly supported by the French Research Ministry under Contract No. 92B0472. The Laboratoire d'Optique Quantique is Laboratoire propre du Centre National de la Recherche Scientifique.

[1] J. K. Furdyna, J. Appl. Phys. **64**, R29 (1988).
[2] O. Goede and W. Heimbrodt, Phys. Status Solidi B **146**, 11 (1988).
[3] J. A. Gaj, J. Ginter, and R. R. Galazka, Phys. Status Solidi B **89**, 655 (1978).
[4] A. V. Komarov, S. M. Ryabchenko, O. V. Terletskii, I. I. Zheru, and R. D. Ivanchuk, Sov. Phys. JETP **46**, 318 (1977).
[5] J. A. Gaj, R. R. Galazka, and M. Nawrocki, Solid State Commun. **25**, 193 (1978).
[6] A. E. Turner, R. L. Gunshor, and S. Dutta, Appl. Opt. **22**, 3152 (1983).
[7] D. U. Bartholomew, J. K. Furdyna, and A. K. Ramdas, Phys. Rev. B **34**, 6943 (1986).
[8] M. A. Buttler, Solid State Commun. **62**, 45 (1987).
[9] P. P. Vatamanyuk, A. V. Savitskii, A. I. Savchuk, and K. S. Ul'yanitskii, Sov. Phys. JETP **67**, 2084 (1988).
[10] H. J. Jiménez-González, R. L. Aggarwal, and P. Becla, Phys. Rev. B **45**, 14011 (1992).
[11] I. M. Boswara, R. E. Howard, and A. B. Lidiard, Proc. R. Soc. London Ser. A **269**, 125 (1962).
[12] L. Roth, Phys. Rev. **133**, A542 (1964).
[13] M. Balkanski, E. Amzallag, and D. Langer, J. Phys. Chem. Solids **27**, 299 (1966).
[14] A. K. Bhattacharjee, Phys. Rev. B **41**, 5696 (1990); in *Proceedings of the 20th International Conference on the Physics of Semiconductors,* edited by E. M. Anastassakis and J. D. Yoannopoulos (World Scientific, Singapore, 1990), Vol. 1, p. 763.
[15] See, for instance, W. J. Tabor, in *Laser Handbook,* edited by F. T. Arecchi and E. O. Schulz-Dubois (North-Holland, Amsterdam, 1972), Vol. 1.
[16] See, for instance, C. Flytzanis, in *Quantum Electronics,* edited by H. Rabin and C. L. Tang (Academic, New York, 1975), Vol. 1, Pt. A.
[17] See, for instance, C. Kittel, *Introduction to Solid State Physics,* 3rd ed. (Wiley, New York, 1968).
[18] R. J. Elliot, T. P. McLean, and G. G. MacFarlane, Proc. Phys. Soc. **72**, 553; Proc. Phys. Soc. **73**, 976 (1959).
[19] J. A. Gaj, R. Planel, and G. Fishman, Solid State Commun. **29**, 435 (1979).
[20] D. Coquillat, J. P. Lascaray, M. C. Desjardins-Deruelle, J. A. Gaj, and R. Triboulet, Solid State Commun. **59**, 25 (1986).

[21]B. M. Askerov, T. G. Ismailov, and M. A. Mekhrabova, Phys. Status Solidi B **163**, K117 (1991).
[22]J. Spalek, A. Lewicki, Z. Tarnawsky, J. K. Furdyna, R. R. Galazka, and Z. Obuszko, Phys. Rev. B **33**, 3407 (1986).
[23]R. Triboulet, A. Heurtel, and J. Rioux, J. Cryst. Growth **101**, 131 (1990).
[24]J. Y. Huang, J. Y. Zhang, Y. R. Shen, C. Chen, and B. Wu, Appl. Phys. Lett. **57**, 1961 (1990).
[25]Y. R. Lee and A. K. Ramdas, Solid State Commun. **51**, 861 (1984).
[26]Atsuko Ebina, Takao Ko, and Shigeo Shionoya, J. Phys. Chem. Solids **26**, 1497 (1965).
[27]Y. R. Lee and A. K. Ramdas, Bull. Am. Phys. Soc. **30**, 214 (1985).
[28]M. C. Desjardins-Deruelle, J. P. Lascaray, D. Coquillat, and R. Triboulet, Phys. Status Solidi B **135**, 227 (1986).
[29]D. Coquillat, J. P. Lascaray, J. A. Gaj, J. Desportes, and J. K. Furdyna, Phys. Rev. B **39**, 10 088 (1989).